International Journal of Engineering Trends and Technology
ISSN: 2231–5381 / https://doi.org/10.14445/22315381/IJETT-V72I10P103

Volume 72 Issue 10, 21-34, October 2024

Review Article

Removal of Mercury Ions from Wastewater Using Different Techniques

Ho Soon Min[1], Subhajit Ray[2]

[1]*Faculty of Health and Life Sciences, INTI International University, Putra Nilai, Negeri Sembilan, Malaysia.*
[2]*Department of Food Engineering & Technology, Central Institute of Technology Kokrajhar, (Deemed to be University, MoE, Gov. of India), Kokrajhar, BTAD, Assam, India*

[1]*Corresponding Author : soonmin.ho@newinti.edu.my*

Received: 03 May 2024 Revised: 07 August 2024 Accepted: 20 September 2024 Published: 25 October 2024

Abstract *- Mercury ion is highly toxic and can be observed in living organisms. It is nondegradable, resulting in several diseases even at low concentrations. Wastewater treatment is very important to ensure good quality of water. Water pollution should be solved by using different techniques. Adsorption as a unit operation process is basically defined as the surface phenomenon involving the separation of materials on a solid matrix. Activated carbon (as adsorbent) will be prepared using carbonaceous materials through carbonization, and activation process. Experimental results confirmed that the obtained carbons are well-developed porosity structures with higher surface area. Adsorption equilibrium, thermodynamics, and kinetics were studied. Research findings highlighted that the adsorption capacity is strongly affected by different conditions. The percentage of removal should be improved from time to time to ensure that pollutants can be eliminated successfully.*

Keywords *- Wastewater treatment, Water pollution, Water purification, Water use, Activated carbon, Adsorbent.*

1. Introduction

Adsorption as a unit operation process is basically defined as the surface phenomenon involving the partitioning of materials onto a solid matrix. Surface energy is the driving force of this phase separation operation. The phase that results in adsorption is known as adsorbent, and the substance absorbed by that material is termed adsorbate [1]. The adsorption phenomenon can be categorized into two processes, namely physisorption and chemisorption. Physisorption is due to the weak Vanderwall's forces and electrostatic forces of attraction between adsorbate and adsorbent [2]. Strong chemical forces between adsorbate and adsorbent cause chemisorption. Different factors such as surface area, temperature, pressure [3], and the nature of adsorbing material affect both physisorption and chemical adsorption. The adsorption capacity of adsorbent [4] is solely dependent upon specific surface area and microporosity. Polar adsorbents such as zeolite, porous alumina, silica gel, and silica-alumina are generally hydrophilic. However, non-polar adsorbents, including activated carbon [5], activated clay, impregnated carbons, polymer adsorbents, and silicalite, are generally lyophilic. The adsorption process is very useful [6] in various industrial operations, such as the purification of waters and wastewater and the removal of undesirable pigments or colorants in edible oil refineries, drugs, and pharmaceutical industries. Activated carbon is generally considered a suitable nonpolar adsorbent [7]. It could be prepared using carbonaceous materials such as coconut shells, coal, wood, apples, olives, potatoes, and orange peels. The efficiency of absorptivity mainly depends upon a larger surface area [8], a higher degree of porosity [9], surface activity, chemical inertness [10], and thermal stability [11]. Various forms of activated carbon are available, such as Biological Activated Carbon (BAC), powdered activated carbon [12], and granulated activated carbon [13]. Biologically activated carbon has been established [14] as a suitable agent for the treatment of wastewater. Powdered activated carbon has been a potential adsorbent for the treatment of nonbiodegradable organic compounds [15] in wastewater treatment plants. Granulated activated carbon loaded packed-bed columns [16] have a significant adsorptive capacity for taste and odor producing compounds in the water treatment process [17].

Activated carbon and its chemically modified form can be efficiently employed in water purification [18] or the removal of heavy metals [19]. Mercury (Hg) is considered a highly toxic substance. It comes from different sources, such as oil refineries, fertilizer industries, chloralkaline wastewater, rubber processing, power generation plants, paper and pulp production. Mercury ion causes chronic and acute toxicity even at low concentrations. It could enter the human body via several ways (pulmonary inhalation, gastrointestinal absorption process, and skin contact). It will

be stored in kidneys, nervous systems, and lung tissues, resulting in several diseases (intestinal dysfunction of the nervous system, paralysis, and urinary complexation). Therefore, the maximum acceptable level (1 μgHg/L) and discharge limit (10 μgHg/L) were highlighted based on the US Environmental Protection Agency.

Table 1. The concentration of mercury in water from different parts of the globe

	Mercury concentration in water (ng/L)
Seawater	
Baltic Sea	0.6
North Sea	0.56
Bothnian Bay	2-40
Gulf of Finland	10-140
River	
Gosku Delta, Turkey	156-1502
Tapajos River, Brazil	0.28-13.3
Ebro Delta, Spain	1-18
Rivers in Wisconsin-industrial area, USA	1-43
Lake	
Lake Michigan, USA	0.3-182
Interstitial	
St. Lawrence Estuary	3.3-15.6

Table 2. The concentration of mercury in precipitation from different parts of the globe

	Mercury concentration in water (ng/L)
Mace Head, Ireland	5.1-37.8
Michigan, USA	1.2-60
Sylt Island, Germany	6.1-18.3
Experimental Lakes area-Ontario, Canada	0.95-9.3
Maine, USA	8.9
Florida, USA	5-113
Hoyama, Japan	5-187

Table 3. The concentration of mercury in bottom sediments from different parts of the globe

	Mercury concentration in water (ng/L)
Sea	
Gulf of Gdansk	3.5
Ninety Mile Beach, Victoria, Australia	290
Baltic Proper	100
La Zacatecana Dam, Mexico	38-790
Danish Strait	60-220
China Sea, Malaysia	20-127
Puck Bay	0.74-2.8
Gulf of Riga	30-790
Mediterranean Sea, Italy	100-5330
The Beagle Channel, Argentina	10-410
Rivers and estuaries	
Goksu Delta, Turkey	594-1152
Odra River, Poland	200-3900
Ebro Delta, Spain	14-185
Nile Delta, Egypt	822
Elba River, Germany	110-12000
Cato Ridge River, South Africa	30-1764000
Scheldt Estuary, Belgium	30-1756
Newark Estuary, USA	380-29600
Anadyr Estuary, Russia	83-2100
Vistula Estuary, Poland	54

Tables 1, 2, and 3 show the mercury concentration in water, precipitation, and bottom sediments from different parts of the globe, respectively. These countries such as Malaysia, Spain, Japan, Germany, Russia, Turkey, the USA, Australia, Poland, Italy, Egypt, Argentina, Finland, and Canada.

This work reviews the removal of mercury ions using different techniques. Mercury ions are toxic substances that must be removed to ensure good quality water. Adsorption capacity was studied under different experimental conditions. Adsorption data was investigated as well.

2. Removal of Mercury Using Activated Carbon

Activated carbon could be considered a cheaper adsorbent if compared to other, more complex water purification technologies. Corn cob-based activated carbon [20] was used to produce activated carbon by means of the carbonization process and chemical activation. In the scanning electron microscopy images (Figure 1), different morphologies could be observed in unmodified activated carbon (no obvious pore structure), modified with potassium hydroxide (many pore structures), and potassium permanganate (a lot of oxygen containing function groups). It was noted that white substances can be found after the adsorption process. According to EDX analysis, the presence of different elements could be detected in KOH (carbon, mercury, and oxygen) and $KMnO_4$ modified activated carbon (carbon, mercury, oxygen, and manganese). It was noticed that adsorption capacity increases when the activation temperature is increased. The highest capacity was 180.02 mg/g at 800 °C due to the reaction rate being increased. The presence of potassium hydroxide will develop the pore structure, creating a large amount of micropores (Table 4) and mesopores as well. However, the specific surface is reduced when the activation temperature is above 800 °C. On the other hand, higher adsorption capacity was reported in potassium permanganate treated activated carbon due to more oxygen containing groups being created. Experimental results confirmed that the highest removal rate was 88.89%, and the maximum adsorption capacity reached 222.2 mg/g for $KMnO_4$ treated carbon (concentration=0.14 mol/L) if compared to activated carbon (without $KMnO_4$). However, researchers suggested that the oxidation process led to a reduction of the adsorption capacity when the concentration of $KMnO_4$ is higher. The adsorption process was mainly monolayer chemisorption according to the obtained experimental findings. The highest correlation coefficients were found in the Langmuir model (R^2>0.978) and pseudo second order isotherm (R^2>0.99), respectively.

Table 4. Properties of corn cob based activated carbon, $KMnO_4$ and KOH treated activated carbon

	Corn cob activated carbon	Potassium permanganate ($KMnO_4$) treated activated carbon	Potassium hydroxide (KOH) treated activated carbon
Surface area (m^2/g)	11.16	1212.93	2797.75
Total volume (cm^3/g)	0.003	1.36	0.59
Micropore volume (cm^3/g)	0.002	0.16	1.16
pHPZC	2.03	Less than 2	3.49

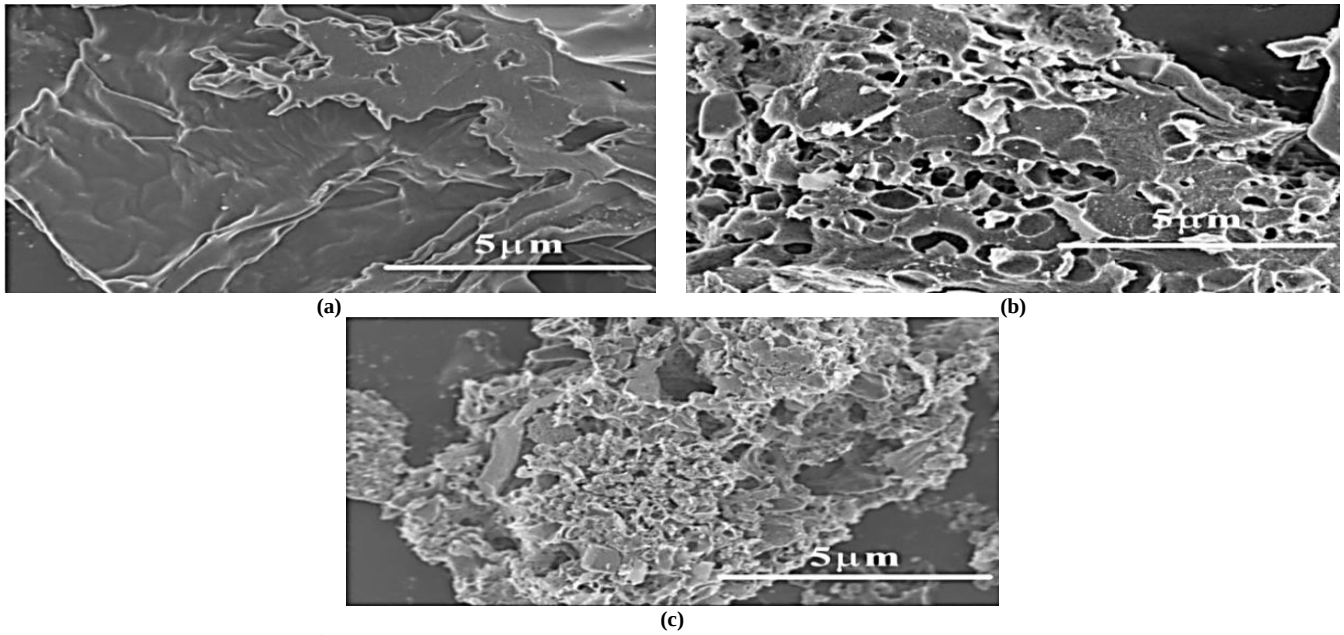

(a) (b) (c)

Fig. 1 SEM images of (a) Corn cob based activated carbon, (b) KOHactivated carbon (c) $KMnO_4$-activated carbon [20]

Iranian walnut shell based activated carbons were employed for absorbing mercury ions from industrial liquid streams [21]. The precursor was collected, dried, and impregnated with zinc chloride for at least 5 hours. Then, these impregnated samples were put in a tubular furnace for the carbonization process under nitrogen conditions. Physical properties such as surface area (780 m^2/g), microporous density (0.45 g/cm^3), and iodine number (737 mg/g) were determined. Researchers have revealed that the surface charge greatly affects the adsorption process. Removal efficiency decreases when the pH is increased. Adsorption data followed the Freundlich model, Langmuir model, and pseudo-second order isotherm. It was also known that the highest adsorption capacity reached 151.5 mg/g (pH=5, particle size=0.088mm).

Ammonium nitrate (activating agent) is used to synthesize pistachio wood based activated carbon via a chemical activation process [22]. Iran is one of the largest global pistachio manufacturing countries. Pistachio wood consisted of cellulose (40-45%), extractives (1-5%), ligwoods (25-30%) and hemicelluloses (20-30%). This activated carbon showed a higher surface area (1448 m^2/g) and total pore volume (0.901 cm^3/g) due to the movement of gases into lignocellulose when the activation process was carried out. The highest adsorption capacity (202 mg/g) was obtained in the best conditions (pyrolysis temperature=800 °C, impregnation ratio=5%, pyrolysis time=120 minutes). Experimental findings concluded that the adsorption process achieved equilibrium within 30 minutes, and the adsorption mechanism was controlled by adsorbent and adsorbate dispersion interactions. Fir wood sawdust based activated carbon [23] has been produced through a chemical activation process (phosphoric acid). The highest surface area (1789 m^2/g) was developed using 1.5g/g of phosphoric acid, while the mesoporous structure was generated with 2g/g of phosphoric acid. It is recognized that removal efficiency increases when pH (2 to pH 8) and adsorbent dosage (0.25 to 2 g/L) are increased. Adsorption data perfectly matched with the pseudo-second order model and Redlich-Peterson isotherm. In the column mode studies, adsorption capacity was described using Yan and Thomas models. While, in the batch investigations, the highest adsorption capacity was 107 mg/g when the impregnation ratio was 1.5 g/g. The number of waste tires has increased sharply annually. Technically speaking, it is very hard to compress and requires a huge amount of environmental space, resulting in new types of pollution. Waste tires contain many carbon contents, and pore structure will be created by proper activation process [24].

Sulfur free rubber materials were used to prepare activated carbon. The optimized pH values were pH 5.5 to pH 6 for excellent mercury removal. Mercury uptake could be defined via rate limiting step, representing the shifting of mercury through pores in the adsorbent. Municipal sewage sludge was collected from the Yamazaki Sewage Sludge Disposal Plant, Nagoya, Japan [25]. It consists of 6.1% hydrogen, 39.4% carbon, 4.46% nitrogen, 2.48% silicon, 1.61% phosphorus and 1.93 sulfur. The carbonization process was carried out in a quartz tube under specific conditions (heating rate=10 °C/min, duration=1 hour, temperature=650 °C, nitrogen flow rate=300 mL/min). The properties of the prepared activated carbon using zinc chloride, phosphoric acid, and sulfuric acid were highlighted (Table 5). Mercury removal using these samples is pH dependent. Adsorption capacity increases when the pH is increased from pH 1 to pH 5. In the adsorption kinetic studies, the highest mercury adsorption capability in zinc chloride treated activated carbon because of higher surface area and larger micropore volume.

However, a longer time is needed to achieve the equilibrium process in this sample (420 minutes) if compared to sulfuric acid (300 minutes) and phosphoric acid treated activated carbon. Also, a lower adsorption rate could be confirmed through Lagergren first order rate equation. The lowest adsorption rate constant (K_{ad}) was observed (K_{ad}=0.008 min^{-1}) compared to other samples. On the other hand, adsorption isotherms have been examined using 120 mg/L of mercury at 25 °C. Experimental findings displayed that higher correlation coefficient (R^2) value in the Freundlich model. Higher adsorption capacity (K_F=42.6 mg/g) and the smallest adsorption intensity (1/n=0.32) were stated. Desorption investigations clarified that 60% to 80% can be recovered in all samples. Bituminous coal was utilized to synthesize granular activated carbon [26] with specific sizes (850 μm to 1180 μm). Average density and BET surface area were estimated to be 1150 kg/m^3 and 850-900 m^2/g, respectively. According to elemental studies, ash content was 9.5%. Ash contained 71% silicon, 20% aluminium, and minor percentages of sodium, titanium, iron, potassium, magnesium, and calcium. Prepared samples indicated slightly basic conditions, and the pH_{pzc} was 8. Adsorption capacity decreases when the temperature is increased in mercury nitrate solution (at pH=2). In acidic conditions, Hg^{2+} ions were found and hydrolyzed to $HgOH^+$ ions when the pH was increased gradually. Obviously, the concentration of Hg^{2+} ions decrease, but $HgOH^+$ ions increase at higher temperatures.

On the other hand, they declared that adsorption capacity increases (more than 25 °C) in mercury chloride solution for pH=7. The most common ions were found to be $HgCl^+$, $HgCl^-_3$, $HgCl^{2-}_4$ ions in acidic conditions, and $HgOH^-_3$ ions at basic pH based on the speciation analysis. Low ash content (Table 6) and mineral content were identified in furfural [27]. Mercury ions sorption by using these adsorbents was confirmed according to experimental results. The Lagergren model fits well, as reported. The adsorption rate constant is reduced (0.193/min to 0.097/min) when the concentration of Hg^{2+} ion is increased (10-40 mg/L) because of the saturation

of the adsorption site. The adsorption process matched the Langmuir model (adsorption capacity=174 mg/g) and Freundlich isotherm as well. Mercury uptakes increased when the pH was increased because of oxygen containing groups (phenolic, carboxylic, hydroxyl, carbonylic, and C_xSO_3H group). The percentage of recovery was 6% based on desorption investigations (treated with hot water).

Mango seed was impregnated [28] with sulfuric acid and calcium chloride for 2 days at 358K. Carbonization was performed in the Carbolite transverse furnace through specific conditions (nitrogen flow rate=80 cm^3/min, heating rate=1 K/min, time=120 minutes, temperature=723 K). It was expressed that the content of volatile matter in raw mango seed was about 74%; however, it dropped to 29%-32% after the carbonization and activation process. It is interesting to mention that lower ash content is compared to other lignocellulosic precursors (up to 26%).

Making a comparison between $CaCl_2$ and H_2SO_4, higher surface area (Table 7) and pore volume could be outlined when $CaCl_2$ is used. Sulfuric acid is a strong dehydrating agent that can break down the lignocellulosic material easily, resulting in the collapse of the structure produced a lower surface area. Research findings pointed out that functionalization and activation processes enhanced more surface groups.

Total acidity has increased by 57% and 90% in $CaCl_2$ treated and sulfuric acid treated activated carbon, respectively, due to the enrichment of the chemical surface with sulfur groups (sulfones or sulfoxides). Adsorption data supported by the Freundlich model (R^2=0.982-0.995), representing multilayer adsorption process. The highest adsorption capacity was 85.6 mg/g (functionalized sulfuric acid treated sample) if compared to other samples because of different textural characteristics.

Table 5. Properties of the organic sewage sludge based activated carbon and adsorption constants for the removal of mercury ions

	No activation treatment	Sulfuric acid activation treatment	Phosphoric acid activation treatment	Zinc chloride activation treatment
Surface area (m^2/g)	137	408	289	555
Micropore volume (cm^3/g)	0.016	0.02	0.053	0.079
Total pore volume (cm^3/g)	0.227	0.523	0.436	0.752
Average pore diameter (nm)	6.65	5.21	2.65	2.26
pH_{zpc}	5.38	4.26	4.12	4.89

Table 6. Characteristics of furfural based activated carbon

Parameter	Results
Moisture	2.5%
Surface area	1100 m^2/g
Ash	0.12%
Micropore volume	0.425 m^3/g
Carbon	88.57%
Macropore volume	0.285 m^3/g
Hydrogen	0.84%
Iodine number	1000 mg/g
Sulfur	0.29%
Mesopore volume	0.11 m^3/g
Nitrogen	0.2%
Oxygen	10.1%
pH	8.6

Table 7. Properties of mango seed based activated carbon

	7% Calcium chloride	15% Sulfuric acid
Moisture (%)	8.2	8.2
Phenolic group (mmol/g)	3.852	2.142
Volatile matter (%)	29	32
Total basicity (mmol/g)	1.739	0.365
Ash (%)	0.9	1.4
Fixed carbon (%)	61.9	58.4
Total acidity (mmol/g)	2.84	2.424
surface area (m^2/g)	33	12
Pore volume (cm^3/g)	0.019	0.006
Lactone group (mmol/g)	1.318	0.219
pH_{pzc}	6.7	5.4
Carboxylic group (mmol/g)	0.305	0.5

Dates nut was cleaned [29] and dried before the carbonization process (300 °C-400 °C) using a muffle furnace. Further, these samples were sieved (90 microns) and activated for 120 minutes using nitric acid solution at 80 °C.

Percentage removal increases when the contact time and adsorbent dose are increased, but the initial concentration is reduced.

Adsorption data were studied using different isotherms (Table 8). According to the Langmuir model, the separation factor was 0.276 (favorable adsorption process) with an adsorption capacity of 1.169 mg/g, respectively. Rate determining steps were controlled by intra-particle diffusion.

Table 8. Kinetics and adsorption data of mercury ions

Model	Results
Freundlich model:	
Slope (1/n) -intensity of adsorption	0.613
K-value (adsorption capacity)	0.582
Correlation coefficient	0.897
Langmuir model:	
Q_0 (adsorption capacity)	1.169 mg/g
B (surface energy)	2.62 L/mg
R_L (separation factor)	0.276
Correlation coefficient	0.943
Lagergren equation:	
Correlation coefficient	0.887
K value	0.063/min
Bhattacharya and Venkobachar equation:	
Correlation coefficient	0.887
K value	0.063
Intra particle diffusion equation:	
Correlation coefficient	0.968
Intercept	3.294
K_p-intra-particle diffusion rate constant	0.235 $mgg^{-1}min^{1/2}$

Commercial activated carbon was prepared by Jacobi Carbons Company using bituminous coal through steam activation [30]. Main characteristics such as surface area (828 m^2/g), particle diameter (0.853 mm-1.2 mm), hardness (95%), and bulk density (0.47 g/cm^3) were interpreted. The synthesis of sulfurized adsorbents has attained great attention, as reported by many researchers. The sample will be impregnated in sulfur containing solutions such as Na_2S, CS_2, Dimethyl disulfide, K_2S, SO_2, and H_2S. Sulfur impregnation was carried out using sulfur dioxide (in nitrogen) through a fluidized bed furnace. The adsorption capacity was improved successfully (about 50%) in specific conditions (temperature=700 °C, sulfurization time=60 minutes, percentage of sulfur=11%) if compared to other samples. It was noted that severe carbon burning could be observed when the temperature was more than 700 °C. Experimental results indicated that adsorption capacity was improved significantly when the time was increased from 30 minutes to 60 minutes. However, less than 2 mg/g adsorption capacity was observed at longer time (3 hours). Based on the adsorbent characterization studies [31], higher pore volume (approximately six times) in sulfur impregnated activated carbon if compared to commercial activated carbon (prepared from Calgon Corporation). Surface area and sulfur content were found to be 610 m^2/g and 13.9%, respectively. Removal of Hg^{2+} ions decreases when the ionic strength has increased and more natural organic matter. Empty fruit bunches were chosen as raw materials because of the abundance of agricultural wastes and the lack of high cellulosic fiber [32]. These precursors were cleaned and dried completely before the carbonization process was conducted (carbonization temperature=400 °C, time=30 minutes).

Table 9. Properties of empty fruit bunches based on activated carbon

Properties	Results
Moisture content	6.3 %
Volatile matter content	8.1%
Ash content	5.5%
Fixed carbon	80.1%
Carbon content	82.96%
Hydrogen content	0.25%
Nitrogen content	0.43%
Surface area	379.37 m^2/g
Apparent density	0.21 g/cm^3

Prepared activated carbon showed higher carbon content (Table 9) but lower nitrogen content because of high carbonization temperature and loss of amine and amide groups, respectively. Removal of volatile matter occurs through the activation process and carbonization reaction, resulting in high porosity will be created. Several peaks, such as 2359 cm^{-1} (C=N stretching) and 1000-1300 cm^{-1} (C-O stretching), could be detected in FTIR studies. Removal of mercury ions was considered as a heterogeneous reaction, as highlighted in the Freundlich model (R^2=0.927). It is noticed that the percentage of removal can reach 100% using 0.2 g adsorbent. More active sites will be developed when the adsorbent dose has increased. In XPS analysis, binding energies of oxygen, nitrogen, and sulfur increase in mercury sorbed modified activated carbon. However, chlorine was unable to be detected, maybe below the detection limit. Activated carbon was purchased from Norit Darco Corporation [33]. Modified activated carbon was prepared using nitric acid, thionyl chloride, and ethylenediamine. Elemental studies confirmed that sulfur and nitrogen content have been increased significantly in modified activated carbon (Table 10). According to the x-ray photoelectron spectroscopy technique, binding energy (O_{1s}, N_{1s}, and S_{2p}) increases on the modified activated carbon as well.

Table 10. Properties of commercial activated carbon

	Commercial activated carbon	Modified activated carbon	Mercury sorbed modified activated carbon
Elemental composition			
Carbon	76.54%	65.86%	
Hydrogen	0.79%	2.23%	
Nitrogen	2.1%	10.29%	
sulfur	0.83%	1.09%	
XPS studies (eV)			
O_{1s}		532.5	533
N_{1s}		400.5	400.58
C_{1s}		285.5	285.5
S_{2p}		160.5	168.5
Hg_{4f}		--	102.5

A faster and higher adsorption rates were detected in modified activated carbon due to the high affinity of surface (ligands) to mercury ions. Adsorption data were defined using the Freundlich model (R^2=0.9123) when the concentration of mercury was high. These adsorbents displayed wider pH values (pH 4-10) and larger removal capacity (95%) if compared to commercial activated carbon. Based on the Langmuir model, adsorption capacity reached 60.08 mg/g with a correlation coefficient of 0.9494 in commercial activated carbon. The walnut shell was washed (remove impurities), dried overnight, and sieved (0.8 mm to 1 mm). One step chemical activation was performed [34] through sodium thiosulfate solution and the impregnation process (4-5 hours). Different morphologies were pointed out before (structural deformation) and after (formation of deep pits) the chemical modification process, as indicated in SEM images. The nitrogen (N_2) adsorption/desorption isotherm summarized that surface area, total pore volume, and average pore diameter were found to be 451.1 m^2/g, 0.303 cm^3/g, and 2.68 nm, respectively, in sodium thiosulfate treated activated carbon. Further, carbon, oxygen, sodium, and sulphur content were identified as 79.26%, 8.92%, 1.43%, and 10.44%, respectively, as shown in Energy-dispersive X-ray spectroscopy elemental mapping. The adsorption process strongly depends on the pH values, representing active site could be protonated and deprotonated. It is noticed that adsorption capacity increases (12.89 to 20.2 mg/g) with increasing pH (2.6 to pH 6.9). Experimental findings revealed that the point of zero charge was 6.1. Obviously, adsorption capacity decreases when the pH is greater than 8 because mercury hydroxide will be formed in alkaline conditions. The highest correlation was observed in the Freundlich model and the maximum capacity (164.4 mg/g) in Langmuir isotherm. The chemisorption process is confirmed through a pseudo second order kinetic model with the lowest chi-squared value. In the thermodynamic parameter studies, spontaneous process (ΔG=-31223 kJ/mol), endothermic reaction (ΔH=32.76 kJ/mol), and degree of freedom increases (ΔS=195.6 J/mol.K) were interpreted during the adsorption process. Birch wood based activated carbon [35] has been synthesized via the phosphoric acid activation process in different gaseous atmospheres. Well-developed porosity structure (Table 11) with the highest surface area (1360 m^2/g) for sample prepared via steam pyrolysis. Also, the steam pyrolysis process enhanced deeper carbonization, resulting in reducing the oxygen and hydrogen content. However, a much smaller surface area and pore volume were observed in the presence of nitrogen gas. Further, the smallest pH (pH=4.5) and the lowest basic groups were highlighted. Experimental results declared that most of the mercury ions had been removed within 20 minutes. However, 10-20 minutes and 30-40 minutes are required for lower and higher concentrations of mercury ions. Adsorption capacity achieved 160 mg/g as expressed using Langmuir model (R^2=0.99967) in specific experimental conditions (impregnation ratio=1.5, adsorbent dose=10 mg/50mL, contact time=60 minutes, atmosphere=steam, concentration of mercury=10-40 mg/L). Based on the previous results, several types of precursors were used to produce activated carbon and eventually to adsorb mercury ions (Table 12). The selection of precursors is affected by production cost, availability, activation agents, and the desired properties of the adsorbents.

Table 11. Properties of birch wood based activated carbon

Properties	Nitrogen	Steam	Nitrogen and Steam
Iodine number (mg/g)	900	1280	1200
Total pore volume (cm^3/g)	0.618	1.026	0.939
Ash (%)	5.61	3.36	3.36
Total mesopore volume (cm^3/g)	0.321	0.541	0.468
Chemical composition:			
Carbon	86.33	92.43	94.84
Hydrogen	2.77	1.80	1.48
Nitrogen	0.2	0.2	0.2
Phosphorus	2.2	0.07	0.14
Oxygen	8.5	5.5	3.34
Surface area (m^2/g)	761	1360	1290
pH	4.5	6.5	5.9
Basic functional groups (meq/g)	0.083	0.902	1.1
Total microvolume (cm^3/g)	0.297	0.485	0.471
Acidic functional group ((meq/g):			
Carboxyl	0.744	N/A	0.124
Lactonic	0.126	0.123	0.034
Hydroxyl	0.48	0.422	0.572
Carbonyl	2.234	2.255	2.53
mean mesopore radius (nm)	1.6	1.5	1.5

Table 12. Removal of mercury ion by activated carbon

Adsorbent	Results	References
Sago wastes	Langmuir model: adsorption capacity=55.6 mg/g, R^2=0.9999. Freundlich model: R^2=0.9839 Conditions: pH=5, particle size=125-250 μm.	Kadirvelu et al., 2004 [36]
Coirpith carbon	The percentage of removal increases when pH increases (pH 2 to 5) and remains constant until pH 11. Langmuir model: adsorption capacity=154 mg/g	Namasivayam and Kadirvelu, 1999 [37]
bagasse pith	isotherms adsorption: Langmuir model, pseudo-second order kinetic isotherm The best pH value was observed to be 4-9 and 6-9 in sulphurised carbon and sulphur free carbon, respectively.	Anoop and Anirudhan, 2002 [38]
Apricot stones, coals, and furfural	Isotherms adsorption: Langmuir model. The percentage of removal increases (pH2-5) is maintained constant until pH 10.	Ekinci et al, 2002 [39]
Ceiba pentandra hulls, Phaseolsaureus hulls, Cicer arietinum waste	Isotherms adsorption: Pseudo-second order-kinetic model, Freundlich isotherm *C. Pentandra* hulls: Removal capacity=25.88 mg/g *P. Aureus* hulls: Removal capacity=23.66 mg/g *C. Arietinum* waste: Removal capacity=22.88 mg/g	Rao et al., 2009 [40]
Peanut hull	Bicarbonate treated peanut hull based activated carbon indicated 7 times more effectiveness if compared to commercial activated carbon. Removal of 20 mg/dm^3 using 70 mg activated carbon could be discovered in specific pH values (pH 3.5 to 10). The adsorption process could be determined using Langmuir and Freundlich model.	Namasivyam and Periasamy, 1993 [41]
Pistachio-nut shells and Licorice residues	Chemical activation was conducted using a zinc chloride solution. Mesoporous porosity with an average pore diameter of 3 nm. The hysteresis loop could be accessed in the N_2 adsorption desorption studies. Adsorption data were evaluated using the Freundlich model and Dubinin-Redushkevich model. Chemisorption reaction is confirmed using pseudo second order kinetics.	Neda et al., 2012 [42]
T. catappa	Isotherms adsorption: Pseudo-second order-kinetic model, Langmuir isotherm Adsorption capacity=94.43 mg/g Conditions: particle size=180-210 μm, pH=5. Thermodynamic studies: endothermic, spontaneous, increased randomness. The highest uptake was 30 mg/L using 4g/L of adsorbent.	Inbaraj and Sulochana, 2006 [43]
Bambusa vulgaris var. striata	Carbonization (furnace, 500 °C, 120 minutes, flow rate of nitrogen=200 mL/min) and activation process (NaOH: charcoal was 3:1) were carried out. Surface area=1041.7 m^2/g Total pore volume=0.622 cm^3/g Average pore diameter=2.39 nm The highest adsorption capacity was 218.08 mg/g, as mentioned using the Thomas model.	Eka et al., 2019 [44]
Nipa palm shell wastes	NaOH treated activated carbon: pore volume=0.758 cm^3/g, surface area=1214 m^2/g. Adsorption capacity reached 227.86 mg/g because of negative surface charges and highly active sides.	Mariana et al., 2023 [45]

3. Removal of Mercury Using Other Techniques

Bio-precipitation of mercury ions through culture off-gas [46] from aerobic Klebsiella pneumoniae M426. It is known that bacteria formed H_2S, to precipitate mercury ions (more than 99 %) within 120 minutes. The obtained materials contain sulfur, carbon, and mercury based on energy-dispersive X-ray microanalysis results. On the other hand, 1,3-benzenediamidoethanethiol is used to offer long-term stability (ligand metal complexes) during the experiment.

Experimental results [47] show that the percentage of removal reached 99.97% when the pH was pH 6. The precipitation technique is fast and favorable to removing mercury ions (large volume), especially in lower concentrations. Farhad and co-workers [48] announced that the highest efficiency was 89% from oil-field brine (injection time=20 minutes, pH=10, reactant concentration=0.5 moles).

Phragmites karka is a reed grass that can be found in tropical regions. Natural form was collected from Lahore, Pakistan [49]. For treatment purposes, the sample will be soaked in $CaCl_2$, ethanol, and NaOH solution. Both samples show the highest adsorption capacity at pH 4, 313 K. The best contact time and agitation speed were reported for natural biosorbent (50 min & 150 rpm) and treated biosorbent (40 min & 100 rpm), respectively. In thermodynamic investigations, adsorption reaction is endothermic (ΔH=24.034 to 26.688 kJ/mol), spontaneous (Δ=-3.058 to -6.573 kJ/mol), and feasible (ΔS=94.62 to 101.69 J/mol.K). Chemisorption can control the biosorption process as confirmed through the pseudo second order kinetic model (R^2>0.994) for both samples representing. Higher adsorption capacity could be found in treated adsorbent (2.268 mg/g) if compared to natural adsorbent (1.787 mg/g), as shown in the Langmuir model. CeO_2 is a better co-catalyst, converting mercury to oxidized mercury in low oxygen conditions [50]. Surface area (232.11 m^2/g), pore volume (0.39 cm^3/g), and pore size (6.38 nm) have been studied in manganese-cerium-aluminium oxide catalysts. In the SEM images, a floc-like structure can be detected after adding cerium and manganese. This structure can enhance the contact area between mercury and catalysts. According to XPS analysis, Mn^{4+} is reduced to Mn^{3+}, Mn^{2+}, and Ce^{4+} converted to Ce^{3+} in the oxidation process. According to experiment findings, removal efficiency reached 48% under pure nitrogen conditions. Further, efficiency increases when 5% oxygen is added, representing lattice oxygen was promoted. On the other hand, removal efficiency was 93% when the time was 140 minutes, at 150 °C. However, removal efficiency decreases at 200 °C and longer times. Thiol membranes can be used to absorb mercury ions due to thiol bonding to ionic mercury to form mercury sulfur complexes. During the formation of the thiol membrane, cysteine and cysteamine will be incorporated into polyacrylic acid functional polyvinylidene fluoride membranes. It is noticed that HgS nanoparticles can be removed (less than 2 ppb) for up to 12.5 hours [51]. In long-term investigations, adsorption efficiency was 97% when the operation time was more than 20 hours. However, adsorption efficiency decreases by using cysteamine membrane (82%) and cysteine membrane (40%) after the addition of calcium ions. The presence of a carboxyl group in the cysteine membrane may affect the adsorption capacity due to the multi-cation adsorption process. Pore functionalized membranes with a chelate group allow the removal of mercury ions through convective flow conditions [52]. Experimental findings indicated that higher adsorption capacity (1015 mg/g) could be found in 1-ethyl-3-(3-dimethylamino) propyl carbodiimide/N-hydroxysuccinimide coupling if compared to ion exchange method (2446 mg/g).

Experimental findings proved that mercury removal from the energy and mining industry was carried out using cysteamine-immobilized polyvinylidene fluoride-poly (acrylic acid) membranes. Based on the fluorescence labelling, the entire porous structure has been functionalized by thiol groups. In membrane technology, several types of polymers (Table 13) have been used to remove mercury ions. The percentage of removal reached about 99% based on the experimental results. Microfiltration, ultrafiltration, and nanofiltration [60] have been used to remove mercury (less than 1.3 ng/L) from oil refinery effluents. A lower operating pressure (2.8 bar) is required for microfiltration and ultrafiltration, while a higher operating pressure (20.7 bar) is required for nanofiltration. It has been verified that more than 90% of mercury can be removed in smaller pore sizes (<0.45 μm). Recent studies confirmed that membrane separation technology requires more operational cost [61]. Because pressure will be supplied for the ultrafiltration process, other disadvantages, such as scale up complexity and high energy, are needed, and other researchers highlighted fouling issues. Pollutants will be collected through the root of the plant in the phytoremediation process, eventually accumulated in plant tissue or converted into less harmful materials. It is an inexpensive method, environmentally friendly and called remediation in situ technique. Researchers have commented that several bacteria can be used to bind mercury. Removal of mercury from sediments and soils was carried out using Nicotiana tabacum L (Solanaceae), tobacco, and Arabidopsis thaliana Thal (Brassicaceae). Methylmercury is called an environmental toxicant and can be found in seafood, leading to neurological degeneration in humans, birds, and cats. Methylmercury was converted to sulfhydryl-bound Hg (II) via bacterial organomercurial lyase gene (merB). Also, a modified bacterial gene (merBpe) using Arabidopsis thaliana plant has been reported to degrade methylmercury [62]. Hg (II) ions decompose to Hg ions through the bacterial mercuric reductase gene (merA). Also, Liriodendron tulipifera, L. (Magnoliaceae), and hybrid willows (Salix spp) showed 10 times faster and the best recovery of mercury (42%), respectively, using merBpe genes.

Azolla caroliniana can be found in sluggish waters, and it is small and native to tropical regions. It is employed as food, biological pesticide, biogas, and hydrogen fuel. Researchers have highlighted that this plant can remove radioactive (uranium), nitrogen, phosphorus, sulfa drugs, chromium, strontium, copper, cadmium, zinc, lead, nickel, and platinum. Removal of mercury ions using Azolla caroliniana from municipal wastewater has been mentioned by Bennicelli and co-workers [63]. Experimental findings confirmed that this plant can accumulate a huge quantity of toxic material. It was noted that the significant differences were less than 0.001 for mercury ions based on statistical data analysis. Also, a higher correlation value (R^2=0.998) between accumulated mercury in plants and applied doses could be observed. Ultrasound promoted reduction/volatilization process [64] has been used to remove mercury ions (trace level). This process consisted of a sono reactor (20 kHz frequency, 100 W power) incorporated formic acid solution. The benefits of this method were that it did not produce any foreign substances. However, the main issue was removal of mercury was affected by oxidants and stabilizing anions. In the reduction mechanism, carbon monoxide and hydrogen will be generated after the decomposition of formic acid. Experimental results showed that 100 ng/mL of mercury can be removed within 0.5 hours and reached 90% from 10 mL water [65]. Sandra and co-workers [66] have observed that the formation of Hg (0) will be prevented by adding permanganate or dichromate anions, and the stabilization of Hg (II) ions will be enhanced after the addition of chloride ions. During the preparation works, nitric acid washing and thermal desorption (370K to 620K) were described [67]. A higher percentage of removal was found at 570 K (90%-99%) than at 370 K (30%-40%) for silica, alumina, and heat-treated dredging sludge samples.

Table 13. Removal of mercury using different membrane technologies

Membrane technology	Percentage of removal (%)	Conditions	References
Polymer enhanced ultrafiltration	99	Polymer: Polyvinylamine Temperature: Room temperature Pressure: 0.2 MPa Flow rate: 60 L/h	Huang et al., 2015 [53].
PEUF	90	Temperature: Room temperature Pressure: 0.2 MPa Flow rate: 65 L/h Polymer: Polyethylenimine, Polyvinylamine, and Poly (acrylic acid)	Huang et al., 2016 [54]
PEUF	99.7	Pressure: 4 bar Temperature: 25 to 30 °C Polymer: polyvinylamine	Barron et al., 2004 [55]
FO	98.2 with sodium chloride 99 with magnesium chloride	pH: 4 to 9 temperature: 25 to 60 °C	Wu et al., 2016 [56]
UF supported with FeS	99	pH: 8 polymer: none temperature: room temperature pressure: 1 bar	Han et al., 2014 [57]
PEUF		Polymer: polyacrylic acid Pressure: 22.2 kPa pH: 5 to 7.5 Flow rate: 60 L/h Temperature: 25 °C	Zeng et al., 2009 [58]
Inorganic/organic nanofibers	97.78 to 99.41	Polymer: polyvinyl alcohol pH: 2 to 12 temperature: room temperature	Tahvili et al., 2019 [59]

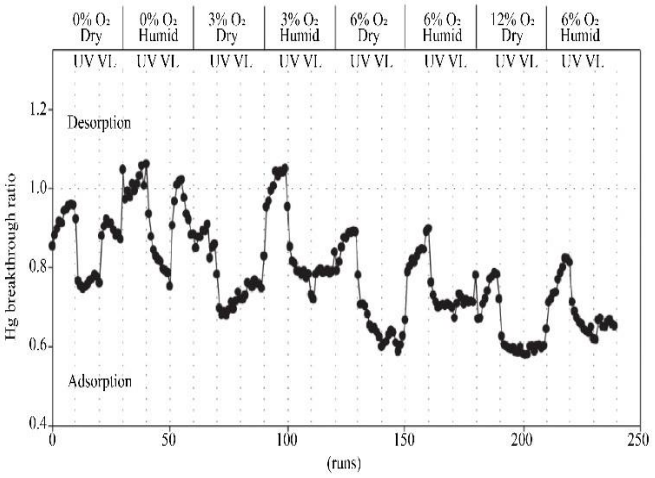

Fig. 2 Mercury breakthrough ratio of Al-doped TiO_2 in various test conditions [69]

The obtained results confirmed that thermal extraction was enhanced (25%) in specific temperatures such as 470K to 520 K. Removal of mercury by using ozone and bromine was reported [68]. Experimental findings indicated that oxygen radicals produced bromine, and BrO radicals improved the adsorption reaction after adding NO. The percentage of efficiency reached 90% by introducing bromine (0.68 ppmv) with ozone (101 ppmv). Al-doped titanium dioxide nanoparticles [69] showed a mixture of rutile and anatase structure with a specific size of 10-105 nm. It was noticed that mercury capture is less effective in the dark, dry, and in the absence of oxygen conditions (Figure 2). The percentage of mercury capture increases when visible light irradiation is used. On the other hand, water will be absorbed into active sites. Mercury capture decreases in humid conditions.

4. Conclusion

Mercury is a toxic substance, resulting in tremors, behavioral abnormalities, vision, and hearing loss. Mercury can be detected in chlor-alkali industries and other plants. In this work, several types of techniques have been reported to adsorb mercury ions from wastewater. As demonstrated by many researchers, adsorption capacity could be enhanced through surface modifications of activated carbon. Adsorption data was studied using different isotherms and can be described using the Langmuir, Freundlich, or Temkin model.

Funding Statement

One of the authors (Ho SM) was supported by INTI International University, Malaysia.

Acknowledgments

This research work was financially supported by INTI International University (Ho SM).

References

[1] Binbin Wu et al., "Adsorption Characteristics of Used Granular Activated Carbon Regenerated by Ultrasonic Backwashing," *Arabian Journal of Chemistry*, vol. 17, no. 4, pp. 1-13, 2024. [CrossRef] [Google Scholar] [Publisher Link]

[2] Yiran Yan et al., "In Situ Production of Bacterial Nanocellulose-Activated Carbon Composites from Pear Juice Industry Wastewater by Two New Komagataeibacter Intermedius and Komagataeibacter Xylinus Isolates for Heavy Metal Removal," *Environmental Technology & Innovation*, vol. 33, pp. 1-13, 2024. [CrossRef] [Google Scholar] [Publisher Link]

[3] Yuting Wang et al., "Comprehensive Carbon Footprint Analysis of Wastewater Treatment: A Case Study of Modified Cyclic Activated Sludge Technology for Low Carbon Source Urban Wastewater Treatment," *Science of the Total Environment*, vol. 923, 2024. [CrossRef] [Google Scholar] [Publisher Link]

[4] Sarah Mushtaq et al., "Utilizing Sludge-Based Activated Carbon for Targeted Leachate Mitigation in Wastewater Treatment," *Environmental Research*, vol. 249, 2024. [CrossRef] [Google Scholar] [Publisher Link]

[5] Weichen Qin et al., "A New Approach of Simultaneous Adsorption and Regeneration of Activated Carbon to Address the Bottlenecks of Pharmaceutical Wastewater Treatment," *Water Research*, vol. 252, 2024. [CrossRef] [Google Scholar] [Publisher Link]

[6] Zainab Y. Atiyah, Shatha K. Muallah, and Ali H. Abbar, "Removal of COD from Petroleum Refinery Wastewater by Adsorption Using Activated Carbon Derived from Avocado Plant," *South African Journal of Chemical Engineering*, vol. 48, no. 1, pp. 1-17, 2024. [CrossRef] [Google Scholar] [Publisher Link]

[7] Asya Drenkova-Tuhtan et al., "Reusable and Inductively Regenerable Magnetic Activated Carbon for Removal of Organic Micropollutants from Secondary Wastewater Effluents," *Water Research*, vol. 255, 2024. [CrossRef] [Google Scholar] [Publisher Link]

[8] Yahnis Dago-Serry et al., "Composite Super-Adsorbents of Chitosan/Activated Carbon for the Removal of Nonsteroidal Anti-Inflammatory Drug from Wastewaters," *Journal of Molecular Structure*, vol. 1298, no. 2, 2024. [CrossRef] [Google Scholar] [Publisher Link]

[9] Jemal Fito Nure et al., "Adsorption of Black MNN Reactive Dye from Tannery Wastewater Using Activated Carbon of Rumex Abysinicus," *Journal of the Taiwan Institute of Chemical Engineers*, vol. 151, pp. 1-20, 2023. [CrossRef] [Google Scholar] [Publisher Link]

[10] Mohammad Almadani, "Adsorption Process Modeling to Reduce COD by Activated Carbon for Wastewater Treatment," *Chemosphere*, vol. 339, 2023. [CrossRef] [Google Scholar] [Publisher Link]

[11] Xiaodan Zhao et al., "Comparison on Molecular Transformation of Dissolved Organic Matter During Fenton and Activated Carbon

Adsorption Processes for Chemical Cleaning Wastewater Treatment," *Separation and Purification Technology*, vol. 344, 2024. [CrossRef] [Google Scholar] [Publisher Link]

[12] Jan Peter Van Der Hoek et al., "Bromate Removal in an Ozone - Granular Activated Carbon Filtration Process for Organic Micropollutants Removal from Wastewater," *Journal of Water Process Engineering*, vol. 58, pp. 1-10, 2024. [CrossRef] [Google Scholar] [Publisher Link]

[13] Jayalakshmi Rajendran et al., "Methylene Blue and Methyl Orange Removal from Wastewater by Magnetic Adsorbent Based on Activated Carbon Synthesised from Watermelon Shell," *Desalination and Water Treatment*, vol. 317, pp. 1-11, 2024. [CrossRef] [Google Scholar] [Publisher Link]

[14] Xiangzhe Jiang et al., "Pilot-Scale Removal of PFAS from Chromium-Plating Wastewater by Anion Exchange Resin and Activated Carbon: Adsorption Difference between PFOS and 6:2 Fluorotelomer Sulfonate," *Chemical Engineering Journal*, vol. 481, 2024. [CrossRef] [Google Scholar] [Publisher Link]

[15] Mina Dolatshah et al., "Development and Modeling of an Integrated Fixed-Film Activated Sludge (IFAS) System for Simultaneous Nitrogen and Carbon Removal from an Industrial Estate Wastewater," *Biotechnology Reports*, vol. 41, pp. 1-16, 2024. [CrossRef] [Google Scholar] [Publisher Link]

[16] Marco Gottardo et al., "A Combined Treatment of Aerobic Activated Sludge and Powdered Activated Carbon: Pilot-Scale Study of Per/Polyfluoroalkyls (PFASs), Organic Matters, Chromium, and Color Removal from Tannery Wastewaters," *Journal of Water Process Engineering*, vol. 55, 2023. [CrossRef] [Google Scholar] [Publisher Link]

[17] Juan Lv et al., "Research on Carbon and Nitrogen Removal of Tetramethylammonium Hydroxide Containing Wastewater by Combined Anaerobic/Integrated Fixed Film Activated Sludge Process," *Chemosphere*, vol. 354, 2024. [CrossRef] [Google Scholar] [Publisher Link]

[18] Jingyu Duan et al., "Enhanced Granulation of Activated Sludge in an Airlift Reactor for Organic Carbon Removal and Ammonia Retention from Industrial Fermentation Wastewater: A Comparative Study," *Water Research*, vol. 251, 2024. [CrossRef] [Google Scholar] [Publisher Link]

[19] Wen-Pei Low et al., "Adsorption of Zinc, Copper, and Iron from Synthetic Wastewater Using Watermelon (Citrullus Lanatus), Mango (Mangifera Indica L.), and Rambutan Peels (Nephelium Lappaceum L.) as Bio-Sorbents," *Journal of Engineering Science and Technology*, vol. 18, no. 1, pp. 386-405, 2023. [Google Scholar] [Publisher Link]

[20] Yuyingnan Liu et al., "Study on Adsorption Properties of Modified Corn Cob Activated Carbon for Mercury Ion," *Energies*, vol. 14, no. 15, pp. 1-22, 2021. [CrossRef] [Google Scholar] [Publisher Link]

[21] M. Zabihi, A. Ahmadpour, and A. Haghighi Asl, "Removal of Mercury from Water by Carbonaceous Sorbents Derived from Walnut Shell," *Journal of Hazardous Materials*, vol. 167, no. 1-3, pp. 230-236, 2009. [CrossRef] [Google Scholar] [Publisher Link]

[22] Seyed-Ali Sajjadi et al., "Efficient Mercury Removal from Wastewater by Pistachio Wood Wastes-Derived Activated Carbon Prepared by Chemical Activation Using a Novel Activating Agent," *Journal of Environmental Management*, vol. 223, pp. 1001-1009, 2018. [CrossRef] [Google Scholar] [Publisher Link]

[23] Fatemeh Kazemi et al., "Thiol-Incorporated Activated Carbon Derived from Fir Wood Sawdust as an Efficient Adsorbent for the Removal of Mercury Ion: Batch and Fixed-Bed Column Studies," *Process Safety and Environmental Protection*, vol. 100, pp. 22-35, 2016. [CrossRef] [Google Scholar] [Publisher Link]

[24] W.R. Knocke, and L.H. Hemphill, "Mercury (II) Sorption by Waste Rubber," *Water Research*, vol. 15, no. 2, pp. 275-282, 1981. [CrossRef] [Google Scholar] [Publisher Link]

[25] Fu-Shen Zhang, Jerome O. Nriagu, and Hideaki Itoh, "Mercury Removal from Water Using Activated Carbons Derived from Organic Sewage Sludge," *Water Research*, vol. 39, no. 2-3, pp. 389-395, 2005. [CrossRef] [Google Scholar] [Publisher Link]

[26] F. Di Natale et al., "Mercury Adsorption on Granular Activated Carbon in Aqueous Solutions Containing Nitrates and Chlorides," *Journal of Hazardous Materials*, vol. 192, no. 3, pp. 1842-1850, 2011. [CrossRef] [Google Scholar] [Publisher Link]

[27] M.F. Yardim, "Removal of Mercury (II) from Aqueous Solution by Activated Carbon Obtained from Furfural," *Chemosphere*, vol. 52, no. 52, pp. 835-841, 2003. [CrossRef] [Google Scholar] [Publisher Link]

[28] Oscar D. Caicedo Salcedo et al., "Study of Mercury [Hg(II)] Adsorption from Aqueous Solution on Functionalized Activated Carbon," *ACS Omega*, vol. 6, no. 18, pp. 11849-11856, 2021. [CrossRef] [Google Scholar] [Publisher Link]

[29] N. Kannan, and S. Malar, "Removal of Mercury (II) Ions by Adsorption onto Dates Nut and Commercial Activated Carbons: A Comparative Study," *Indian Journal of Chemical Technology*, vol. 12, pp. 522-527, 2005. [Google Scholar]

[30] Neda Asasian et al., "Enhanced Mercury Adsorption Capacity by Sulfurization of Activated Carbon with SO_2 in a Bubbling Fluidized Bed Reactor," *Journal of the Taiwan Institute of Chemical Engineers*, vol. 45, no. 4, pp. 1588-1596, 2014. [CrossRef] [Google Scholar] [Publisher Link]

[31] Ke Gai et al., "Impact of Mercury Speciation on its Removal from Water by Activated Carbon and Organoclay," *Water Research*, vol. 157, pp. 600-609, 2019. [CrossRef] [Google Scholar] [Publisher Link]

[32] Rafeah Wahi, Zainab Ngaini, and Veronica Usun Jok, "Removal of Mercury, Lead and Copper from Aqueous Solution by Activated

Carbon of Palm Oil Empty Fruit Bunch," *World Applied Sciences Journal*, vol. 5, pp. 84-91, 2009. [Google Scholar] [Publisher Link]
[33] Jianzhong Zhu et al., "Modifying Activated Carbon with Hybrid Ligands for Enhancing Aqueous Mercury Removal," *Carbon*, vol. 47, pp. 2014-2025, 2009. [CrossRef] [Google Scholar] [Publisher Link]
[34] Hania Albatrni, and Hazim Qiblawey, "Evaluation of Sodium Thiosulfate Activated Carbon for High-Performance Mercury Removal from Aqueous Solutions," *Environmental Technology & Innovation*, vol. 34, pp. 1-14, 2024. [CrossRef] [Google Scholar] [Publisher Link]
[35] T. Budinova et al., "Characterization and Application of Activated Carbon Produced by H_3PO_4 and Water Vapor Activation," *Fuel Processing Technology*, vol. 87, no. 10, pp. 899-905, 2006. [CrossRef] [Google Scholar] [Publisher Link]
[36] K. Kadirvelu, "Mercury (II) Adsorption by Activated Carbon made from Sago Waste," *Carbon*, vol. 42, no. 4, pp. 745-752, 2004. [CrossRef] [Google Scholar] [Publisher Link]
[37] C. Namasivayam, and K. Kadirvelu, "Uptake of Mercury (II) from Wastewater by Activated Carbon from an Unwanted Agricultural Solid by-Product: Coirpith," *Carbon*, vol. 37, no. 1, pp. 79-84, 1999. [CrossRef] [Google Scholar] [Publisher Link]
[38] K. Anoop Krishnan, and T.S. Anirudhan, "Removal of Mercury(II) from Aqueous Solutions and Chlor-Alkali Industry Effluent by Steam Activated and Sulphurised Activated Carbons Prepared from Bagasse Pith: Kinetics and Equilibrium Studies," *Journal of Hazardous Materials*, vol. 92, no. 2, pp. 161-183, 2002. [CrossRef] [Google Scholar] [Publisher Link]
[39] E. Ekinci, and T. Budinova, "Removal of Mercury Ion from Aqueous Solution by Activated Carbons Obtained from Biomass and Coals," *Fuel Processing Technology*, vol. 77-78, pp. 437-443, 2002. [CrossRef] [Google Scholar] [Publisher Link]
[40] M. Madhava Rao et al., "Removal of Mercury from Aqueous Solutions Using Activated Carbon Prepared from Agricultural by-Product/Waste," *Journal of Environmental Management*, vol. 90, no. 1, pp. 634-643, 2009. [CrossRef] [Google Scholar] [Publisher Link]
[41] C. Namasivayam, and K. Periasamy, "Bicarbonate-Treated Peanut Hull Carbon for Mercury (II) Removal from Aqueous Solution," *Water Research*, vol. 27, no. 11, pp. 1663-1668, 1993. [CrossRef] [Google Scholar] [Publisher Link]
[42] Neda Asasian, Tahereh Kaghazchi, and Mansooreh Soleimani, "Elimination of Mercury by Adsorption onto Activated Carbon Prepared from the Biomass Material," *Journal of Industrial and Engineering Chemistry*, vol. 18, no. 1, pp. 283-289, 2012. [CrossRef] [Google Scholar] [Publisher Link]
[43] B. Stephen Inbaraj, and N. Sulochana, "Mercury Adsorption on a Carbon Sorbent Derived from Fruit Shell of Terminalia Catappa," *Journal of Hazardous Materials*, vol. 133, no. 1-3, pp. 283-290, 2006. [CrossRef] [Google Scholar] [Publisher Link]
[44] Eka Marya Mistar, "Adsorption of Mercury(II) Using Activated Carbon Produced from Bambusa Vulgaris Var. Striata in a Fixed-Bed Column," *Sains Malaysiana*, vol. 48, no. 4, pp. 719-725, 2019. [CrossRef] [Google Scholar] [Publisher Link]
[45] Mariana Mariana et al., "Nipa Palm Shell as a Sustainable Precursor for Synthesizing High-Performance Activated Carbon: Characterization and Application for Hg^{2+} Adsorption," *Bioresource Technology Reports*, vol. 21, 2023. [CrossRef] [Google Scholar] [Publisher Link]
[46] Ashraf M.M. Essa, Lynne E. Macaskie, and Nigel L. Brown, "A New Method for Mercury Removal," *Biotechnology Letters*, vol. 27, pp. 1649-1655, 2005. [CrossRef] [Google Scholar] [Publisher Link]
[47] Matthew M. Matlock, Brock S. Howerton, and David A. Atwood, "Irreversible Precipitation of Mercury and Lead," *Journal of Hazardous Materials*, vol. 84, no. 1, pp. 73-82, 2001. [CrossRef] [Google Scholar] [Publisher Link]
[48] Farhad Fazlollahi et al., *Method for Removal of Mercury from Oil Field Brine with Calcium Carbonate Co-Precipitation*, Characterization of Minerals, Metals, and Materials, 2014. [CrossRef] [Google Scholar] [Publisher Link]
[49] Muhammad Hamid Raza et al., "Phragmites Karka as a Biosorbent for the Removal of Mercury Metal Ions from Aqueous Solution: Effect of Modification," *Journal of Chemistry*, vol. 2015, no. 1, pp. 1-12, 2015. [CrossRef] [Google Scholar] [Publisher Link]
[50] Zhong He et al., "Removal of Mercury from Coal-Fired Flue Gas and its Sulfur Tolerance Characteristics by Mn, Ce Modified γ-Al_2O_3 Catalyst," *Journal of Chemistry*, vol. 2020, no. 1, pp. 1-10, 2020. [CrossRef] [Google Scholar] [Publisher Link]
[51] Mohammad Saiful Islam et al., "Mercury Removal from Wastewater Using Cysteamine Functionalized Membranes," *ACS Omega*, vol. 5, no. 35, pp. 22255-22267, 2020. [CrossRef] [Google Scholar] [Publisher Link]
[52] Sebastián Hernández et al., "Thiol-Functionalized Membranes for Mercury Capture from Water," *Industrial & Engineering Chemistry Research*, vol. 59, no. 12, pp. 5287-5295, 2020. [CrossRef] [Google Scholar] [Publisher Link]
[53] Yifeng Huang et al., "Removal of Mercury (II) from Wastewater by Polyvinylamine-Enhanced Ultrafiltration," *Separation and Purification Technology*, vol. 154, pp. 1-10, 2015. [CrossRef] [Google Scholar] [Publisher Link]
[54] Yifeng Huang et al., "Batch Process of Polymer-Enhanced Ultrafiltration to Recover Mercury (II) from Wastewater," *Journal of Membrane Science*, vol. 514, pp. 229-240, 2016. [CrossRef] [Google Scholar] [Publisher Link]
[55] J. Barron-Zambrano et al., "Mercury Removal and Recovery from Aqueous Solutions by Coupled Complexation-Ultrafiltration and Electrolysis," *Journal of Membrane Science*, vol. 229, no. 1-2, pp. 179-186, 2004. [CrossRef] [Google Scholar] [Publisher Link]
[56] Chia-Yu Wu et al., "Removal of Trace-Amount Mercury from Wastewater by Forward Osmosis," *Journal of Water Process Engineering*, vol. 14, pp. 108-116, 2016. [CrossRef] [Google Scholar] [Publisher Link]

[57] Dong Suk Han et al., "Reactive Iron Sulfide (FeS)-Supported Ultrafiltration for Removal of Mercury (Hg(II)) from Water," *Water Research*, vol. 53, pp. 310-321, 2014. [CrossRef] [Google Scholar] [Publisher Link]

[58] Jian Xian Zeng et al., "Selective Separation of Hg(II) and Cd(II) from Aqueous Solutions by Complexation-Ultrafiltration Process," *Chemosphere*, vol. 76, pp. 706-710, 2009. [CrossRef] [Google Scholar] [Publisher Link]

[59] Arash Tahvili et al., "New Efficient Inorganic-Organic Nanofibers Electrospun Membrane for Fluorescence Detection and Removal of Mercury (II) Ions," *Journal of Molecular Structure*, vol. 1179, pp. 242-251, 2019. [CrossRef] [Google Scholar] [Publisher Link]

[60] Meltem Urgun-Demirtas, "Achieving Very Low Mercury Levels in Refinery Wastewater by Membrane Filtration," *Journal of Hazardous Materials*, vol. 215-216, pp. 98-107, 2012. [CrossRef] [Google Scholar] [Publisher Link]

[61] Hania Albatrni, Hazim Qiblawey, and Muftah H. El-Naas, "Comparative Study between Adsorption and Membrane Technologies for the Removal of Mercury," *Separation and Purification Technology*, vol. 257, pp. 1-15, 2021. [CrossRef] [Google Scholar] [Publisher Link]

[62] Scott P. Bizily et al., "Phytoremediation of Methylmercury Pollution: merB Expression in Arabidopsis Thaliana Confers Resistance to Organomercurials," *Proceedings of the National Academy of Sciences*, vol. 96, no. 12, pp. 6808-6813, 1999. [CrossRef] [Google Scholar] [Publisher Link]

[63] R. Bennicelli et al., "The Ability of Azolla Caroliniana to Remove Heavy Metals (Hg(II), Cr(III), Cr(VI)) from Municipal Waste Water," *Chemosphere*, vol. 55, no. 1, pp. 141-146, 2004. [CrossRef] [Google Scholar] [Publisher Link]

[64] Ziqi He et al., "Removal of Mercury from Sediment by Ultrasound Combined with Biomass (Transgenic Chlamydomonas Reinhardtii)," *Chemosphere*, vol. 83, no. 9, pp. 1249-1254, 2011. [CrossRef] [Google Scholar] [Publisher Link]

[65] Sandra Gil, Isela Lavilla, and Carlos Bendicho, "Mercury Removal from Contaminated Water by Ultrasound-Promoted Reduction/Vaporization in a Microscale Reactor," *Ultrasonics Sonochemistry*, vol. 15, no. 3, pp. 212-216, 2008. [CrossRef] [Google Scholar] [Publisher Link]

[66] Sandra GilIsela, LavillaCarlos, and Bendicho, "Ultrasound-Promoted Cold Vapor Generation in the Presence of Formic Acid for Determination of Mercury by Atomic Absorption Spectrometry," *Analytical Chemistry*, vol. 78, no. 17, pp. 6260-6264, 2006. [CrossRef] [Google Scholar] [Publisher Link]

[67] Barbara Lesa et al., "Bench-Scale Tests on Ultrasound-Assisted Acid Washing and Thermal Desorption of Mercury from Dredging Sludge and Other Solid Matrices," *Journal of Hazardous Materials*, vol. 171, no. 1-3, pp. 647-653, 2009. [CrossRef] [Google Scholar] [Publisher Link]

[68] Yaning Sun et al., "Radical-Induced Oxidation Removal of Mercury by Ozone Coupled with Bromine," *ACS ES&T Engineering*, vol. 1, no. 1, pp. 110-116, 2021. [CrossRef] [Google Scholar] [Publisher Link]

[69] Cheng-Yen Tsai, Tien-Ho Kuo, and Hsing-Cheng His, "Fabrication of Al-Doped TiO_2 Visible-Light Photocatalyst for Low-Concentration Mercury Removal," *International Journal of Photoenergy*, vol. 2012, no. 1, pp. 1-8, 2012. [CrossRef] [Google Scholar] [Publisher Link]